SIX DAYS ■ THREE CONFERENCES ■ ONE EXHIBITION

EUROPEAN MICROWAVE WEEK 2018
IFEMA - FERIA DE MADRID, MADRID, SPAIN
23RD - 28TH SEPTEMBER 2018

EuMW2018 PASSION FOR MICROWAVES

EUROPEAN MICROWAVE WEEK
IFEMA FERIA DE MADRID, SPAIN
23-28 SEPTEMBER 2018
www.eumweek.com

EUROPEAN MICROWAVE WEEK 2018

CONFERENCE PROGRAMME

EUROPE'S PREMIER MICROWAVE, RF, WIRELESS AND RADAR EVENT

Register online at:
www.eumweek.com

EuMA
European Microwave Association

Official Publication: Microwave Journal

Organised by: Horizon House

Supported by: IET The Institution of Engineering and Technology

Co-sponsored by: MTT-S

Co-sponsored by: IEEE

EuMIC 2018
The 13th European Microwave Integrated Circuits Conference
Co-sponsored by:

48th European Microwave Conference 2018
The 48th European Microwave Conference
Co-sponsored by: EurAAP

EuRAD 2018
The 15th European Radar Conference
Co-sponsored by: EurAAP AESS

WEDNESDAY

N106	N107	N108	N110
EuMC20 Solid State High Power Amplifiers Chair: Sergio Pires[1] Co-Chair: Philippe Eudeline[2] [1]Ampleon, [2]Thales Air Systems SAS	**EuMC21 Filter Synthesis Techniques** Chair: Richard Snyder[1] Co-Chair: Giuseppe Macchiarella[2] [1]RS Microwave, [2]Politecnico di Milano	**EuMC22 Non-Conventional Designs in Antenna Technology** Chair: David Escot-Bocanegra[2] Co-Chair: Carlos Montesano[1] [1]Airbus DS Space, [2]INTA	**EuMC23 THz Components** Chair: Antti Räisänen[1] Co-Chair: Luis Enrique Garcia-Muñoz[2] [1]Aalto university, [2]Universidad Carlos III de Madrid

08:30 - 08:50

EuMC20-1
Quasi-MMIC High Power Amplifier with Silicon IPD Matching Network
Junhyung Jeong[1], Phirun Kim[1], Phanam Pech[1], Jongsik lim[2], Yongchae Jeong[1]
[1]Chonbuk National University, [2]Soonchunhyang University

EuMC21-1
Lossy Dual-Mode Bandpass Filter With Non-Uniform Q Method
Hongliang Guo[1], Jia Ni[1], Jiasheng Hong[1], Petronilo Martin Iglesias[2]
[1]Heriot-Watt University, [2]European Space Agency, ESA/ESTEC

EuMC22-1
Miniaturization Design of Millimeter Wave Conformal Array Antenna
Jingping Liu[1]
[1]Nanjing University of Science and Technology

EuMC23-1
300-GHz CMOS Receiver Module with WR-3.4 Waveguide Interface
Shinsuke Hara[1], Kyoya Takano[2], Kosuke Katayama[2], Ruibing Dong[2], Koichi Mizuno[3], Kazuaki Takahashi[3], Issei Watanabe[1], Norihiko Sekine[1], Akifumi Kasamatsu[1], Takeshi Yoshida[2], Shuhei Amakawa[2], Minoru Fujishima[2]
[1]National Institute of Information and Communications Technology, [2]Hiroshima University, [3]Panasonic Corporation

08:50 - 09:10

EuMC20-2
New Class-F High Efficiency Multi-Bias Optimised GaN HPA for C-Band Applications
Wilfried Demenitroux[1], Lucas Mandica[1], Nicolas Berthou[1], Frederic Ploneis[1], Audrey Thorinius[2]
[1]Thales Communications & Security, [2]Thales DMS

EuMC21-2
Linear Time-Invariant Behavioral Digital Models of Frequency-Periodic RF/ Microwave Filters
Jose-Maria Munoz-Ferreras[1], Dimitra Psychogiou[2], Roberto Gomez-Garcia[1]
[1]University of Alcala, [2]University of Colorado at Boulder

EuMC22-2
Novel Single/Dual Beam Scanning Provided by an Array Composed of Two CRLH SIW LWAs
Rihem Noumi[1], Jan Machac[2], Ali Gharsallah[1]
[1]Faculty of Sciences of Tunisia, [2]Czech Technical University in Prague

EuMC23-2
Monopulse RLSA Antenna with Gap-Waveguide Feeding Network for Space Debris Radar at 94 GHz
Adrián Tamayo Dominguez[1], José Manuel Fernández-González[1], Manuel Sierra Castañer[1]
[1]Universidad Politécnica de Madrid

09:10 - 09:30

EuMC20-3
Wideband High Efficiency 50 W GaN-HEMT Balanced Power Amplifier
Quang Huy Le[1], Gernot Zimmer[1 2]
[1]Frankfurt University of Applied Sciences, [2]Vietnamese-German University

EuMC21-3
A Theoretical Synthesis of Coupling Matrix by Eigen Mode Expansion Method and Householder Transform
Shigeki Takeda[1], Tetsuo Anada[2], Chun-Ping Chen[2]
[1]Antenna Giken Co., Ltd., [2]Kanagawa University

EuMC22-3
Perforated Rectangular Dielectric Resonator Antenna for Wideband, Dual band and Single band application
Pragati Patel[1], Eeshaan Vernekar[1], Mallikarjun Erramshetty[1]
[1]NIT Goa

EuMC23-3
E-band Radio Fiber as Low-Cost mm-Wave Waveguide Junction
Stefano Moscato[1], Matteo Oldoni[1], Giuseppe Parisi[2]
[1]SIAE Microelettronica, [2]SM-Optics

09:30 - 09:50

EuMC20-4
50% High Efficiency X-Band GaN MMIC Amplifier for Space Applications
Anne-Marie Couturier[1], Nicolas POITRENAUD[1], Véronique SERRU[1], Jean-Jacques FONTECAVE[1], Roberto DIONISIO[2], Marc Camiade[1]
[1]United Monolithic Semiconductors SAS, [2]ESA

EuMC21-4
Application of a Series Open Circuit Stub Transform to Bandpass Filter Design.
Johannes Malherbe[1]
[1]University of Pretoria

EuMC22-4
An Electrical-Contactless Substrate-Over-Waveguide Planar Array Slot Antenna
Alfonso Tomás Muriel-Barrado[1], Manuel Sierra Perez[1], José Manuel Fernández-González[1]
[1]Technical University of Madrid

EuMC23-4
Terahertz Gapless Low Insert Loss Waveguide Switch Technology
Chuxian Zhang[1]
[1]Beijing Aerospace Research Institute of Micro Electrical-Mechanical Technology

09:50 - 10:10

EuMC21-5
Synthesis of Wideband Filters Using Single-Short-Circuited-Stub-Loaded Parallel-Coupled-Lines
Chun-Ping Chen[1], Daisuke Tetsuda[1], Zejun Zhang[1], Tetsuo Anada[1], Shigeki Takeda[2], Zhewang Ma[3], Xiaolong Wang[3]
[1]Kangawa University, [2]Antenna Giken Co., Ltd., [3]Saitama University

EuMC22-5
Compact Cavity-Backed Spiral Antennas with Enhanced Axial Ratio and Gain at Low Frequencies
Andrea García-Estellés[1], Juan José Sánchez-Martínez[1], Ana Cristina Gago-Lancho[1], Francisco Vázquez-Vázquez[1]
[1]Indra Sistemas S.A.

EuMC23-5
THz and Microwave Dual-Band Ultrafast Photoconductive Antenna
Elliott Brown[1], Andrea Mingardi[1], Weidong Zhang[1], Enrique Garcia[2], Guillermo Carpintero[2], Daniel Segovia-Vargas[2]
[1]Wright State University, [2]University Carlos III Madrid

Quasi-MMIC High Power Amplifier with Silicon IPD Matching Network

Junhyung Jeong[#1], Phirun Kim[#], Phanam Pech[#], Yongchae Jeong[#2], and Sangmin Lee[*3]
[#]Division of Electronics and Information Engineering, Chonbuk National University, Republic of Korea
[*]Wavice Inc., Hwasung-si, Republic of Korea
[1]jjunh05@jbnu.ac.kr, [2]ycjeong@jbnu.ac.kr, [3]smlee@wavice.com

Abstract — **In this paper, the quasi-monolithic microwave integrated circuit (MMIC) high power amplifier (HPA) with silicon integrated passive device (IPD) matching network is proposed. The proposed quasi-MMIC HPA consists of commercial GaN transistor power cell and IPD matching network using silicon substrate. The proposed quasi-MMIC HPA can achieve similar output power and efficiency characteristics compared with the conventional MMIC HPAs. Moreover, the manufacturing cost can be reduced due to the silicon substrate process. For experimental validation, the proposed quasi-MMIC HPA was designed and fabricated at the 8.5 GHz for radar application. The measurement results shows that the output power and drain efficiency at saturation point are 48.5 dBm (70.8W) and 45.5%, respectively, with pulse signal test (100 usec pulse width and 10% duty.**

Keywords — **high resistivity silicon, integrated passive device matching network, internally matched, power amplifier, quasi-MMIC, radar.**

I. Introduction

Power amplifier (PA) is an important circuit in RF wireless communication and radar systems. Especially, high power performance of PA is required in military radar systems to increase the detection range. To achieve power requirement, PAs are used in the radar system as shown in Fig.1 because of limited output power capability of transistor. The number of PA/LNA is decided according to number of array antennas and the individual transmitting powers are combined and radiated in array antenna. Also, size and product cost of individual PA are important issues because overall size and cost according to number of array of PAs are increased. Therefore, PA block in radar system should be considered high output power, efficiency, size, and cost simultaneously.

Conventional GaAs monolithic microwave integrated circuit (MMIC) is one of several solutions with high integration level, broadband output, and efficiency performances. Moreover, the design freedom is high because the lumped elements such as resistor, capacitor, and inductor can be easily modeled and used. Nevertheless, power capability of GaAs MMIC is not enough for the radar system. Therefore, GaN-on-SiC MMIC technologies were developed to increase output power in MMIC process [1]-[2]. They consisted of transistor power cell realized with the GaN material and the passive matching network (MN) with MMIC technology on SiC substrate. As using GaN transistor and SiC substrate, high output power and efficiency can be obtained at microwave frequency. And good heat dissipation characteristics are also obtained. However, manufacturing cost

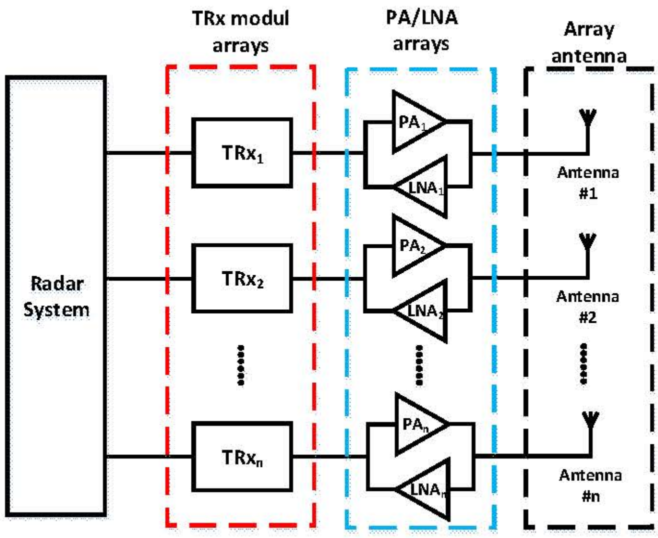

Fig. 1. Block diagram of radar system

and difficulty of process are increased due to the GaN process on SiC substrate.

Another approach is quasi-MMIC structures. The quasi-MMIC structures consisted of the passive MNs realized with high dielectric substrate printed circuit board (PCB) or GaAs MMIC process and the commercial GaN transistor power cell [3]-[6]. Each input/output passive MNs are connected with GaN transistor by bonding wire. However, the manufacturing cost is increased according to the compositions of PCB, the specific material of substrate, and GaAs MMIC process. In case of high dielectric PCB MNs, the design freedom is reduced than conventional MMIC MNs because the lumped elements cannot be implemented in the MN. Moreover, the precise implementation process is required to avoid input/output matching characteristics variation due to the fabrication errors of transmission line and bonding wire.

In this paper, the quasi-MMIC high power amplifier (HPA) with silicon (Si) integrated passive device (IPD) MN is presented. Compared with the conventional quasi-MMIC HPAs, the proposed HPA provides lower manufacturing cost due to the Si substrate. Moreover, the proposed HPA has high integration level passive circuits and the design freedom because the conventional standard Si IPD process techniques can be used. For a validation, the design procedure and experimental results of the quasi-MMIC HPA with Si IPD MN are provided.

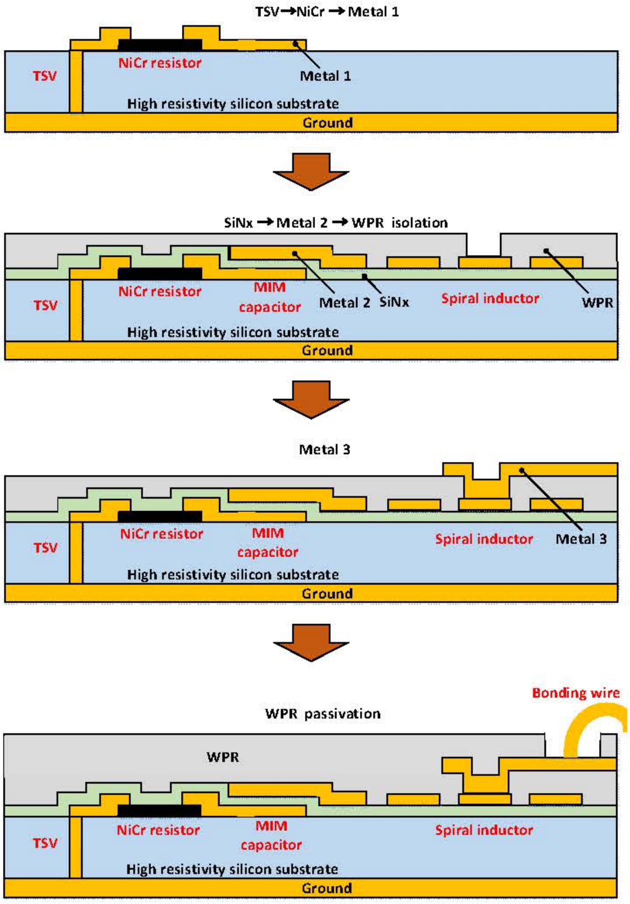

Fig. 2. Passive network fabrication procedure

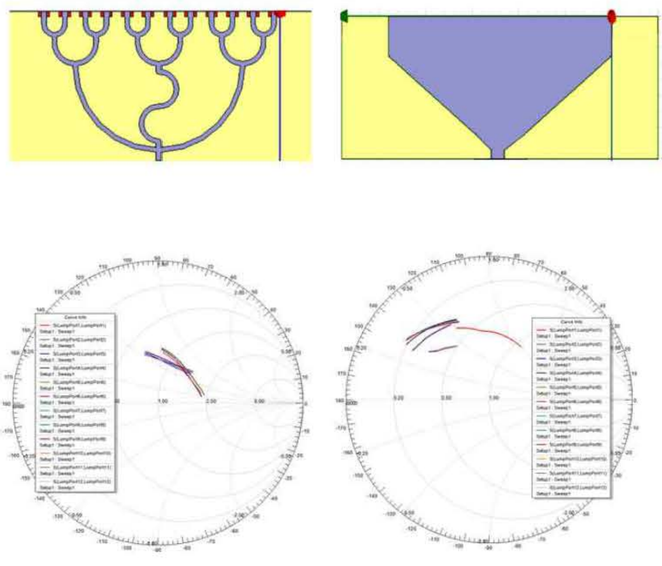

(a) (b)

Fig. 3. Signal transfer characteristics of feeding networks at each transistor pad: (a) signal line circuit and (b) tapper bus structure.

II. A DESIGN OF PROPOSED QUASI-MMIC HPA

This section provides a rough description of the Si IPD process for realizing a passive networks and the actual HPA design procedures. Because the passive circuit of proposed quasi-MMIC HPA can utilize the conventional Si semiconductor process technology, not only thin film *R-L-C* devices but also silicon through via (TSV) can be used.

Fig. 2 shows the implementation example of grounded series *R-L-C* circuit with high resistivity silicon (HRS) substrate. At first the TSV is implemented on the HRS substrate for the ground, and then the resistor is implemented using NiCr and attached on Metal 1 for the connection with signal line. Secondly, SiNx is used to fabricate a dielectric layer for metal-insulator-matal capacitors, and Metal 2 is used to fabricate capacitors and spiral inductors. Then, WPR covers SiNx and Metal 2 areas except some part to connect with Metal 3. Thirdly, the pad for the bonding wire and the signal line to connect the spiral inductor at Metal 2 are realized by top Metal 3. Finally, the WPR passivation is done whole circuit except the pad for the bonding wire. Using this process, input and output MNs can be minimized and implemented using lumped elements and transmission lines on a HRS substrate

The proposed quasi-MMIC HPA was designed using a 70 W pulse mode GaN HEMT transistor (CGHV1J070D) of Wolfspeed at 8.5 GHz (f_0). The selected bias condition was V_{DD} = 48 V, V_{GS} = -2.6 V, and I_{DQ} = 330 mA. As load-pull simulation, the optimum load impedance (Z_{opt}) is 1.46 + j2.2 Ω with saturation output power of 49 dBm. The input matching impedances of transistor at f_0 and $2f_0$ are chosen 2 Ω and 1 + j10 Ω by source-pull simulation.

The used GaN TR has twelve pads at the gate and drain ends, respectively. Therefore, the feeding circuit for connecting each pad to the matching circuit affects circuit characteristics. Fig. 3 shows the signal line circuit (SLC) and tapper bus structure networks and the transfer characteristics from each pad to the output. Whereas the SLC structure shows relatively uniform transfer characteristics than the tapper bus structure, the tapper structure shows several different transfer characteristics according to pad locations. Especially, there is serious difference between the paths through the pads at both ends to the output and the paths through the center pads to the output. Because the signals of individual pads in the SLC structure are sequentially combined, the output powers at all pads are well combined at the final output stage, so that high output power and efficiency are achieved

Fig. 4 show the EM simulation result of the output MN using SLC structure and bonding wire. The load impedance at f_0 is 1.36 + j2.3 Ω for the Z_{opt} point. Even though the harmonic matching circuit is not implemented to reduce the insertion loss of the MN, it shows that the second harmonic ($2f_0$) impedance is matched at the short circuit point due to the shunt parasitic capacitance of the MN with Si substrate. The input MN is also implemented using the same structure.

Fig. 5 shows the measured gain and drain efficiency (DE) of the proposed HPA according to the output power. The measurement results show that the output power and DE are 48.5 dBm, and 45.5%, respectively, at the saturation point with pulse signal (width = 100 usec and duty = 10%). Fig. 6 shows the output power and DE according to the operating frequency. Bandwidth of output power over 60 W is 330 MHz, where DE

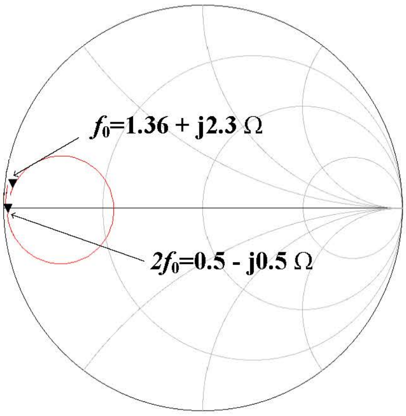

Fig. 4. EM simulation result of designed output matching network.

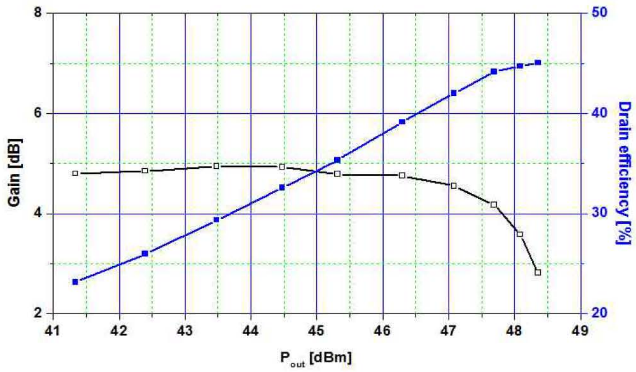

Fig. 5. Measured gain and drain efficiency of quasi-MMIC HPA with Si IPD MN at 8.5 GHz.

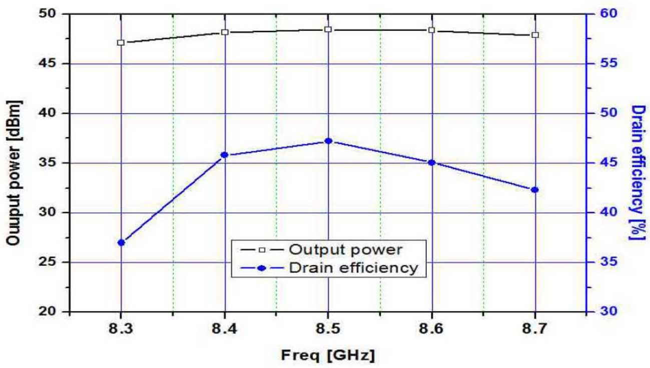

Fig. 6. Frequency characteristics of quasi-MMIC HPA with Si IPD MN.

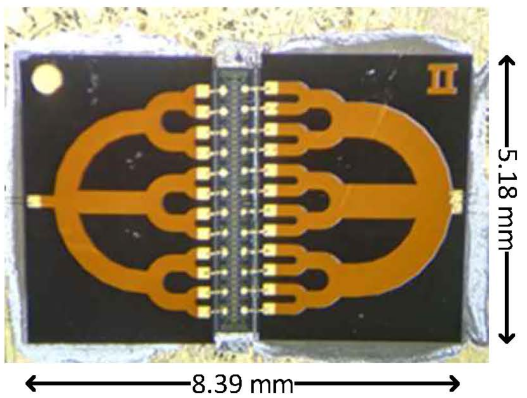

Fig. 7. Photograph of fabricate quasi-MMIC HPA with silicon IPD MN

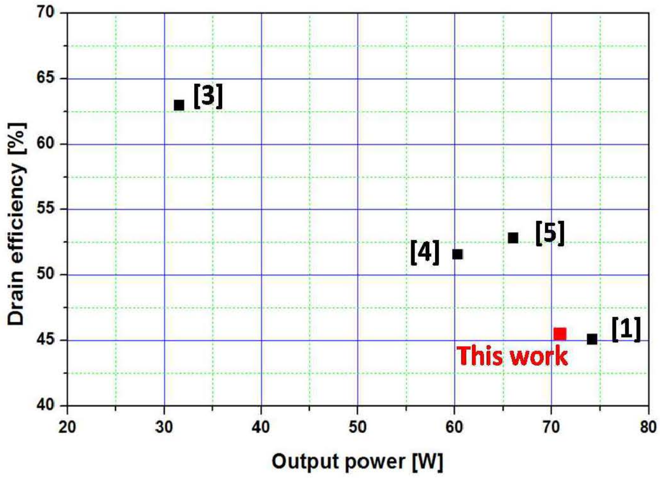

Fig. 8. State-of-art of the drain efficiency versus output power between X-band HPAs

is more than 40%. Fig. 7 is a photograph of quasi-MMIC HPA with Si IPD MN. GaN transistors were eutectic bonded using Au and Si IPD was fixed using silver epoxy. The MN and GaN TR were connected using a 2 mil gold wire whereas the input and output ports were connected to an external circuit using a 1 mil gold wire. The input and output feeds were designed with 100 μm and 200 μm, respectively, to endure supply DC current and high output RF power.

Fig. 6 shows the output power and DE according to the operating frequency. Bandwidth of output power over 60 W is 330 MHz, where DE is more than 40%. Fig. 7 is a photograph of quasi-MMIC HPA with Si IPD MN. GaN transistors were eutectic bonded using Au and Si IPD was fixed using silver epoxy. The MN and GaN TR were connected using a 2 mil gold wire whereas the input and output ports were connected to an external circuit using a 1 mil gold wire. The input and output feeds were designed with 100 μm and 200 μm, respectively, to endure supply DC current and high output RF power.

III. Comparison with Conventional HPAs

In this section, the state-of-art is presented to show that the proposed circuit is suitable for comparison with other X-band HPAs. Table 1 shows the characteristics of the conventional HPA and the proposed quasi-MMIC HPA in the X-band. The proposed circuit has similar or better characteristics compared to the MMIC HPA using SiC substrate. Compared with researches used quasi-MMIC structure, the efficiency is slightly lower but the output power is higher. In the view of size between same structures, the proposed HPA is small relative to the output power. Fig. 8 shows state-of-art with DE efficiency versus output power. It can be seen that the proposed circuit is located together with conventional studies at the lower right side. Therefore, the proposed quasi-MMIC HPA has similar characteristics to those of the conventional studies and has a great advantage in terms of manufacturing cost.

Table 1. Performance comparison with previous works.

Ref.	Freq. [GHz]	Output power [W]	Drain efficiency [%]	Fabrication process	Pulse signal width [usec] / duty [%]	Size [mm²]
[1]	9.2	74.13	45.1*	MMIC (SiC Substrate)	100 / 10	3.5×3.8
[2]	10	13.4	25.7*	MMIC (SiC Substrate)	100 / 10	4.5×3
[3]	10	31.5	63*	Quasi-MMIC (3 kinds PCBs: ε_r=10, 90 and 38)	Non / 10	5.4×3.8
[4]	X-band	60.3	51.57*	Quasi-MMIC (2 kinds PCBs: ε_r=38 and 10)	80 / 10	7×7.7
[5]	9.4	66	52.8*	Quasi-MMIC (ε_r=36)	100 / 10	9.6×8.6
This work	8.5	70.8	45.5	Quasi-MMIC (Si IPD)	100 / 10	8.39×5.18

* calculated value,

IV. Conclusion

In this paper, the quasi-MMIC HPA with silicon (Si) integrated passive device (IPD) matching network (MN) is described. Proposed HPA is used quasi-MMIC structure with standard Si IPD MNs at input/output both sides. For the uniform power transmitting of each pad and effective combination at the output, the signal line circuit feeding structure was used. The fabricated quasi-MMIC HPA with Si IPD MN has high output power and efficiency similar to those of the conventional researches. Therefore, the proposed quasi-MMIC HPA can reduce the manufacturing cost with high output power and efficiency performances and it can be apply to the array radar systems.

Acknowledgment

Research reported in this work has been supported by ICMTC (Institute of Civil-Military Technology Cooperation) of Korea under an ICMTC program (16-CM-SS-16).

References

[1] H. I. Tao, W. Hong, B. Zhang, and X. Yu, "A compact 60W X-band GaN HEMT power amplifier MMIC," *IEEE Microwave Wireless Component Letter*, vol. 27, no. 1, pp. 73-75, Jan. 2017.

[2] F. Van Raay, R. Quay, R. Kiefer, F. Benkhelifa, B. Raynor, W. Pletschen, M. Kuri, H. Massler, S. Müller, M. Dammann, M. Mikulla, M. Schlechtweg, and G. Weimann, "A coplanar X-band AlGaN/GaN power amplifier MMIC on s.i. SiC Substrate," *IEEE Microwave Wireless Component Letter*, vol. 15, no. 7, pp. 460-462, Jul. 2005.

[3] Y. Kawamura, M. Hangai, T. Mizutani, K. Tomiyama, and K. Yamanaka, "30W output / 60% PAE GaN power amplifier at X-band 8% relative bandwidth," *Proceedings of the Asia-Pacific Microwave Conference*, Dec. 2016.

[4] M. Kimura, K. Yamauchi, K. Yamanaka, H. Noto, E. Kuwata, H. Otsuka, A. Inoue, Y. Kamo, and M. Miyazaki, "GaN X-band 43% internally-matched FET with 60W output power," *Proceedings of the Asia-Pacific Microwave Conference*, Dec. 2008.

[5] C. F. Campbell and M. Poulton, "Compact highly integrated X-band power amplifier using commercially available discrete GaN FETs," *Proceedings of the Asia-Pacific Microwave Conference*, Dec. 2011.

[6] M. Camiade, D. Bouw, G. Mouginot, F. Auvray, P. F. Alleaume, D. Floriot, L. Favède, J. Thorpe, and H. Stieglauer, "Highly integrated S and C-band internally-matched quasi-MMIC power GaN devices," *Proceedings of the European Microwave Conference*, Oct. 2012.